Numerical Simulation of Landing Aircraft Dynamics

Zdravko TERZE, *Milan* VRDOLJAK **and** *Hinko* WOLF

Fakultet strojarstva i brodogradnje Sveučilišta u Zagrebu (Faculty of Mechanical Engineering and Naval Architecture, University of Zagreb)
Ivana Lučića 5, HR - 10000 Zagreb
Republic of Croatia

zdravko.terze@fsb.hr

Preliminary note

Numerical simulation procedures for landing dynamics of large transport aircraft are briefly presented. Developed numerical procedures allow for determination of dynamic response of landing aircraft for different flight and touch-down parameters. A non-linear dynamic model of landing aircraft, which serves as a basis for computational procedures, is synthesised by modelling of aircraft structural subsystems using a multibody dynamics approach. A dynamic model with variable kinematical structures includes discontinuous dynamics of landing gear oleo-pneumatic shock-absorber with friction and hydraulic/thermodynamic processes. Non-linear tire contact dynamics and unilateral dynamics of nose gear elastic leg assembly is modelled as well. The longitudinal and lateral aerodynamic loads are estimated by considering various aircraft system configurations (landing gears in "up" and "down" position, different control surfaces in active/inactive modes). A mathematical model is derived as a differential-algebraic (DAE) system. The developed numerical tools are modularly shaped and efficient numerical integration methods as well as original procedures for MBS constraint stabilization are applied for dynamic response determination. On the basis of the presented model, dynamic simulations of landing cases of large transport aircraft were performed for different initial descent velocities with focus on determination of dynamical loading of main landing gear assembly.

Numeričke simulacije dinamike slijetanja zrakoplova

Prethodno priopćenje

U ovom radu ukratko su opisane numeričke simulacijske procedure za dinamiku slijetanja velikog transportnog zrakoplova. Razvijene numeričke procedure omogućavaju određivanje dinamičkog odziva zrakoplova prilikom slijetanja i to za različite parametre leta i slijetanja. Nelinearni dinamički model zrakoplova pri slijetanju, kao osnova računalnih procedura, dobiven je sintezom modela konstrukcijskih podsustava zrakoplova primjenom mehaničkih i matematičkih algoritama dinamike konstrukcijskih sustava. Dinamički model zrakoplova s varijabilnom kinematičkom topologijom obuhvaća diskontinuiranu dinamiku oleo-pneumatske elastične noge glavnog podvozja s uključenim termodinamičkim/hidrauličnim procesima, kontaktnu dinamiku gume te nelinearnu unilateralnu dinamiku elastične noge nosnog kotača. Uzdužna i bočna aerodinamička opterećenja procijenjena su za različite konfiguracije letjelice (uvučeno/izvučeno podvozje, izvučena/uvučena zakrilca te otkloni ostalih upravljačkih površina). Matematički model izveden je kao sustav diferencijalno-algebarskih jednadžbi (DAE). Razvijeni računalni alati oblikovani su modularno te su za potrebe određivanja dinamičkog odziva primijenjene efikasne metode numeričke integracije, kao i originalne procedure stabilizacije dinamičkih odziva konstrukcijskih sustava sa složenim kinematičkim ograničenjima. Temeljem izloženog modela provedene su dinamičke simulacije slijetanja velikog transportnog zrakoplova i to za različite brzine spuštanja s fokusom na određivanje dinamičkog opterećenja glavnog podvozja.

Symbols/Oznake

C_N	- aerodynamic coefficient of normal force
	- aerodinamički koeficijent normalne sile
C_n	- aerodynamic coefficient of yawing moment
	- aerodinamički koeficijent momenta skretanja
F_{gear}	- shock absorber total force, N
	- ukupna sila elastično-prigušnog elementa
i_h	- angle of horizontal tail deflection, rad
	- otklon horizontalnog repa
$\mathcal{M}^n$	- manifold
	- višestrukost
$\begin{matrix} m \\ k \end{matrix}$	- mass of the B_k-th body, kg
	- masa B_k-tog tijela
N	- number of bodies
	- broj tijela
p^*, q^*, r^*	- normalised angular velocity: roll, pitch, yaw
	- normirana kutna brzina: valjanja, propinjanja, skretanja
$R_k^{i\,i}$	- rotation matrix of the B_k-th body
	- matrica rotacije B_k-tog tijela
t	- time, s
	- vrijeme
V	- aerodynamic velocity, m/s
	- aerodinamička brzina

$v_x, v_y, v_z,$	- flight velocity components, m/s
	- komponente brzine leta
$X_k^{(i)}$	- center of gravity coordinates of the B_k-th body, m
	- koordinate središta mase B_k-tog tijela
α	- angle of attack, rad
	- napadni kut
$\ddot{\alpha}^*$	- normalised angle of attack angular velocity
	- normirana kutna brzina
β	- sideslip angle, rad
	- kut klizanja
δ_f	- angle of flaps/slats deflection, rad
	- otklon zakrilaca/pretkrilaca
δ_{gear}	- shock absorber stroke, m
	- ugib elastično-prigušnog elementa
δ_l	- angle of aileron deflection, rad
	- otklon krilaca
δ_m	- angle of elevator deflection, rad
	- otklon kormila visine
δ_n	- angle of rudder deflection, rad
	- otklon kormila pravca
ψ_k^{ij}	- Binet's inertia tensor of the B_k-th body, kg·m²
	- Binetov inercijski tenzor B_k-tog tijela

1. Introduction

During landing and taxiing, a transport aircraft landing gear and parts of an airframe can be exposed to high dynamic loading. In the extreme situations even damages and loss of the stability of an airplane may be expected. During large airplane tail-down landing, all dynamic loads are carried on the main gear first: dynamic characteristics of the main gear are of the most significant importance for the safe touchdown and landing during which airframe load factors should be kept in the prescribed range [1–3]. However, when the aircraft critical landing conditions and structural loads are being determined, the simplifications are often made: aerodynamic loads are oversimplified, aircraft pitching and rolling motion are neglected or tire dynamics and wheel spin-up forces are not taken into consideration [2]. Although some basic characteristics of landing aircraft dynamic response can be determined by linear dynamic analysis [4], dynamic simulation of landing an airplane for the sake of its stability analysis or determination of landing structural loads requires a full-scale non-linear multibody approach.

In the paper, a non-linear dynamic model of a large transport aircraft that allows for dynamic simulation of airplane landing cases is briefly described. The model includes aircraft aerodynamic loads, discontinuous dynamics of shock absorbers oleo-pneumatic elements (main and nose landing gear) and aircraft tires 3D dynamics including longitudinal and lateral loading. Because of its great influence on the aircraft ground dynamic behaviour and structural loads determination, dynamic model of the main gear shock absorber is presented in more detail. Based on the developed model, landing cases of the large transport aircraft for different initial descent velocities are simulated and dynamic landing force and stroke of landing gear shock absorber are presented.

2. Landing aircraft dynamical model

2.1. Multibody dynamical model

The aircraft dynamic model that allows for non-linear dynamic simulation of 3D landing is designed as a multibody system with variable kinematic structures. The "global" model comprises the aircraft main body, main landing gear consisting of two elastic legs with the upper part (upper part of shock absorber + additional masses) and the lower part (lower part of shock absorber + wheel and tire + additional masses) and nose gear consisting of

the upper and lower part of the same structure. The "local" structural subsystems of different parts and mechanisms are independently modelled and incorporated in the "global" scheme (Figure 1).

The gears' upper and lower parts are connected via non-linear force couplers, modelled according to the shock absorbers dynamic characteristics. With this aim in view, the main elastic leg and shock-absorber subassemblies as well as nose gear elastic leg mechanism are modelled in detail using CAD tools (Figure 1, Figure 4). After defining geometry, non-linear models of their dynamic behaviour are numerically tested (Figure 3) and built into the "global" dynamic model.

The additional non-linear force couplers are added to model aircraft's tire dynamics: it is assumed that the aircraft main gear is equipped with four tires of the conventional type and two conventional tires are mounted on the aircraft nose gear. Mechanical properties of the tires are estimated after [5] and manufacturer's

data [6] and the dynamic model considers tire non-linear dynamic behaviour (inertia effects, centrifugal growth of tire radius, side loads). The calculation of tire contact dynamics spin-up force is based on variable slip-friction characteristics and a slippage factor defined according to [6] (Figure 4). It is assumed (and verified by the simulation results) that tire-bottoming deflections will not occur during analysed motion.

Generally, dynamic response of landing aircraft includes unsteady aspects, not only because of the external landing impact, but also with regard to the unilateral contact phenomena within landing gear mechanism. Full 3D aerodynamic loads are estimated by considering various aircraft system configurations (landing gears in up and down position, different control surfaces in active/ inactive modes). The whole aircraft ("global" model) and parts of main shock absorber assembly are depicted in Figure 1.
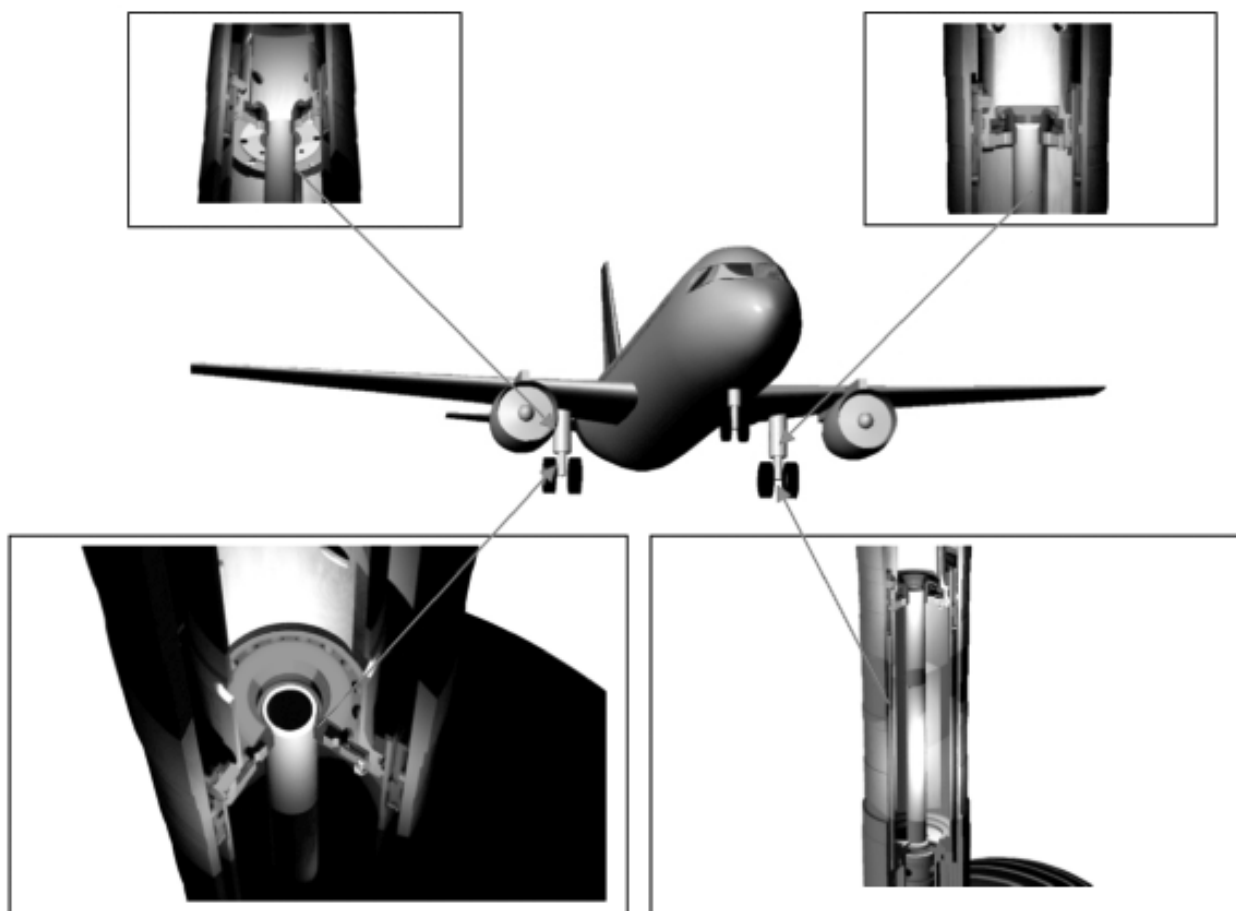
Figure 1. Schematic landing aircraft global multibody model and details of shock absorber assembly model - low pressure gas chamber / oil chamber, upper and lower bearings, systems of orifices.

Slika 1. Shema globalnog 'multibody' modela zrakoplova pri slijetanju s detaljima sklopa modela elastično-prigušnog elementa – komora niskog tlaka / komora s uljem, gornji i donji ležajevi te sustav otvora.

2.2. Mathematical model

The configuration space $\mathcal{R}^n$ of an airborne aircraft is considered to be a manifold $\mathcal{M}^n$ covered by coordinate system (local chart) $\mathbf{q}(t)$ and equipped with Riemannian metrics via system generalized mass $\mathbb{M}(\mathbf{q}) = [M_{ab}]$. The system kinetic energy $Ek(\mathbf{x}, \dot{\mathbf{x}}) : T \mathcal{M}^n \to \mathcal{R}$ is defined on tangent bundle $T \mathcal{M}^n$ covered by the coordinates $(\mathbf{q}, \dot{\mathbf{q}})$: $T \mathcal{M}^n = \{(\mathbf{q}, \dot{\mathbf{q}}) : \mathbf{q} \in \mathcal{M}^n, \dot{\mathbf{q}} \in T_{\mathbf{q}} \mathcal{M}^n\}$ or explicitly $Ek = \frac{1}{2} M_{ab}\dot{q}^a\dot{q}^b$ and manifold kinematic line element is $ds^2 = M_{ab}dq^adq^b$. Consequently, the dynamic equations of the unconstrained system are given in the form:

$$M_{ab}\ddot{q}^{b} + \Gamma_{a,bc}\dot{q}^b\dot{q}^c = F_a (\mathbf{q}, \dot{\mathbf{q}}, t), \tag{1}$$

where generalized mass (metric tensor) is defined as:

$$M_{ab} = \sum_{k=1}^{N}\Big[\underset{k}{m}\, \partial_{q^a}\underset{k}{X^i}\partial_{q^b}\underset{k}{X^i} + \underset{k}{\psi^{ij}}\partial_{q^a}\underset{k}{R^{ii}}\partial_{q^b}\underset{k}{R^{ij}}\Big], \tag{2}$$

and Christoffel symbols of the first kind

$$\Gamma_{a,bc} = \sum_{k=1}^{N}\Big[\underset{k}{m}\, \partial_{q^a}\underset{k}{X^i}\partial_{q^b}\partial_{q^c}\underset{k}{X^i} + \underset{k}{\psi^{ij}}\partial_{q^a}\underset{k}{R^{ii}}\partial_{q^b}\partial_{q^c}\underset{k}{R^{ij}}\Big], \tag{3}$$

define non-linear velocity terms (centrifugal, gyroscopic, Coriolis); symmetric Riemannian connection on $\mathcal{M}^n$ is defined by $\Gamma^a_{bc} = M^{ad}\Gamma_{d,bc}$. Inertial frame $\mathcal{E}^3$ coordinates of mass centre of the body B_k (N, number of bodies) are given by $\underset{k}{X^i}$. Mass and Binet's inertia tensor of the body B_k are $\underset{k}{m}$ and $\underset{k}{\psi^{ij}}$ and $\underset{k}{R^{ij}}$ is the rotation matrix of the body, where underlined indices refer to the inertial frame; generalized applied forces are given by F_a. By imposing a system of kinematic constraints (landing gear external contacts, elastic leg extension constraints [7]):

$$\mathbf{\Phi}(\mathbf{q}, t) = \mathbf{0}, \quad \mathbf{\Phi}(\mathbf{q}, t) : \mathcal{R}^n \times \mathcal{R} \to \mathcal{R}^r, \tag{4}$$

the system is forced to move on the configuration submanifold:

$$\mathcal{S}^{n-r}(t) = \{\mathbf{q} \in \mathcal{M}^n, \mathbf{\Phi}(\mathbf{q}, t) = \mathbf{0}\},$$

and velocities and accelerations of the system are given by:

$$\mathbf{\Phi}_{\mathbf{q}}(\mathbf{q}, t)\dot{\mathbf{q}} = -\mathbf{\Phi}_t, \tag{5}$$

$$\mathbf{\Phi}_{\mathbf{q}}(\mathbf{q}, t)\ddot{\mathbf{q}} = \xi. \tag{6}$$

The mathematical model of the aircraft multibody system is shaped as a differential-algebraic system (DAE) of index 1 (redundant coordinates formulation) [8], where Lagrangian equations of the first type (7) and the kinematic constraint equations at the acceleration level (8) are put together in matrix form:

$$\mathbb{M}(\mathbf{q})\ddot{\mathbf{q}} + \mathbf{\Phi}_{\mathbf{q}}^{\mathrm{T}}(\mathbf{q}, t) = \mathbf{Q}(\mathbf{q}, \dot{\mathbf{q}}, t), \tag{7}$$

$$\mathbf{\Phi}_{\mathbf{q}}(\mathbf{q}, t)\ddot{\mathbf{q}} = \xi. \tag{8}$$

$\mathbb{M}(\mathbf{q})$ is positive-definite inertia matrix, $\mathbf{\Phi}_{\mathbf{q}}(\mathbf{q}, t)$ is the system's Jacobian (kinematical constraint matrix) and $\mathbf{Q}(\dot{\mathbf{q}}, \mathbf{q}, t)$ represents the applied forces and centrifugal and gyroscopic terms [8-7]. Since the system has variable kinematic configuration (during motion several kinematic constraints change form active to inactive mode and reverse), it is integrated using DAE numerical routines and constraint violation stabilization procedures [8].

2.3. Aerodynamic model

Aerodynamic loads in the dynamic simulation of landing transport aircraft are defined with an aerodynamic model. In a general case, this model consists of three forces and three moments written in the form of aerodynamic coefficients needed for the description of longitudinal and lateral aircraft motion. These aerodynamic coefficients are estimated for the transport aircraft [9] according to datasheet component built-up methods, as for example [10].

In order to fully describe the aerodynamic loads for landing aircraft it is necessary to analyze different aircraft configuration with respect to the landing gear position, flaps and slats deflection. A linear aerodynamic model is assumed since the angle of attack α and side slip angle β are within a linear domain. For example aerodynamic coefficient of normal force has the following form:

$$C_{\mathrm{N}} = C_{\mathrm{N0}}(\delta_\mathrm{f}) + C_{\mathrm{N\alpha}}(\delta_\mathrm{f})\alpha + C_{\mathrm{Nq}}q^* + C_{\mathrm{N\dot\alpha}}\dot\alpha^* + C_{\mathrm{N\delta m}}\delta_\mathrm{m} + C_{\mathrm{Nih}}i_\mathrm{h}$$

and aerodynamic coefficient of the yawing moment is:

$$C_{\mathrm{n}} = C_{\mathrm{n\beta}}(\delta_\mathrm{f})\beta + C_{\mathrm{np}}p^* + C_{\mathrm{nr}}r^* + C_{\mathrm{n\delta l}}\delta_1 + C_{\mathrm{n\delta n}}\delta_\mathrm{n}.$$

Here p^*, q^*, r^*, α^* present non-dimensional aircraft angular velocities, δ_l, δ_m, δ_n, i_h, deflections of control surfaces and δ_f deflection of flaps/slats.

Aerodynamic model, with defined mass properties of the aircraft, is used for dynamic simulation of the aircraft in landing approach in order to define initial conditions for dynamical response determination of the aircraft multibody model for touch-down and taxiing. Results of the dynamic simulation for one landing case ending with the touch-down are given in Figure 2.

The same aerodynamic model is used in the aircraft multibody simulation phase after the touch-down, with the addition of ground effects and spoiler deflection.

Landing approach / Zalaz za slijetanje
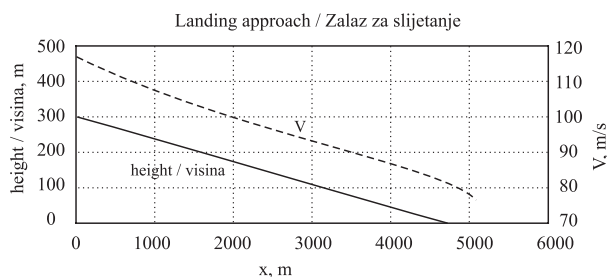
Figure 2. Approach profile and aircraft velocity during the landing approach.

Slika 2. Profil prilaza pri slijetanju i brzina letjelice tijekom zalaza za slijetanje.

3. Landing gear shock absorber

Most commonly, a telescopic main landing gear of a transport aircraft comprises a shock absorber of oleo-pneumatic type [6, 11]. Considering a contemporary design, it is a several stage unit and contains four chambers: a first-stage oleo-pneumatic chamber containing low pressure gas and hydraulic fluid, a recoil chamber and compression chamber containing hydraulic fluid and a second-stage pneumatic chamber that contains high pressure gas (nitrogen) (Figure 3).
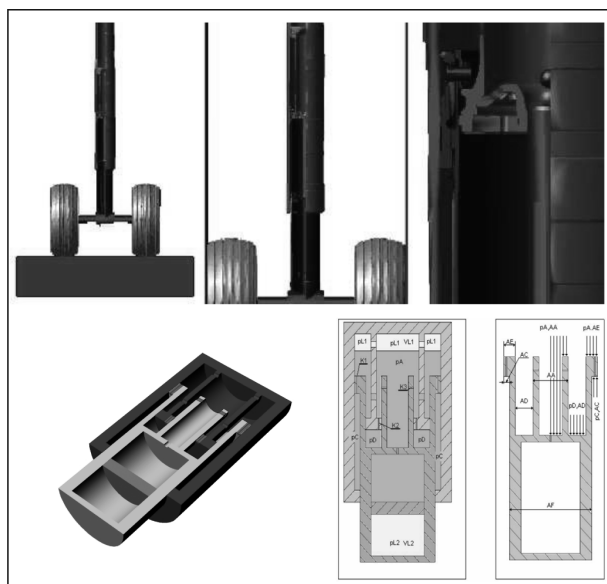
Figure 3. Main landing gear elastic leg multibody model and schematic oleo-pneumatic shock absorber. The animation of dynamic simulation of "drop-test" - numerical testing of elastic leg dynamic characteristics and data validation (JAR-25).

Slika 3. Model elastične noge glavnog podvozja i shema oleo-pneumatskog prigušnog elementa. Animacija dinamičke simulacije "drop-test-a" – numerički pokus određivanja dinamičkih značajki elastične noge i provjera rezultata (JAR-25).

The floating piston in the second-stage cylinder separates hydraulic fluid and high pressured nitrogen. During a compression stroke, the floating piston does not become active until the gas pressures of the first-stage and second-stage chambers are equal, which happens during the system's increased dynamic loading. Dynamic characteristics of the shock absorber are strongly influenced by the systems of orifices that control a hydraulic flow and by means of which net hydraulic resistance can be tuned. Considering different possibilities of the activation of a floating piston and orifices as the absorber closes, it can be shown that four operation stages can be identified during the compression stroke.

During the return stroke, primary control of the shock absorber recoil consists of the fluid flow from the recoil chamber into the oleo-pneumatic chamber and from the oleo-pneumatic chamber to the compression chamber. To prevent unit (and airplane!) excessive rebound, the orifices hydraulic resistance increases significantly during the absorber recoil stroke.

3.1. Dynamical model

Since mechanical properties of the landing gear shock absorber are mainly determined by the pneumatic spring force and oleo (hydraulic) damping force, dynamic model of the absorber are presented in the overall multibody system as a force coupling element (highly non-linear!) consisting of these terms. All mechanical characteristics and geometrical data (AA, AC, AD etc., Figure 3) needed to establish the mathematical model are determined on the basis of CAD modelling according to [6]. The cylinder-piston stick-slip friction phenomenon and internal seal friction are also introduced. The floating piston inertia effect is neglected in the absorber dynamic model presented here.

3.1.1. Pneumatic spring force

Depending on the unit operation stage, the pneumatic spring force is defined by the initial inflation pressure in two nitrogen chambers and by the change of volume of the shock absorber (unit current kinematical configuration).

During modelling, instantaneous gas compression ratio in accordance with the polytrophic law for compression [12-13] is assumed. Since an absorber high rate of compression is to occur during landing impact, the polytrophic exponential term is chosen as $n = 1,3$ during modelling of all internal processes [14]. Having considered the geometrical determinations of the gas chambers (volumes VL1, VL2, Figure 3.) depending on the unit kinematic configuration and after determination of initial gas inflation pressure [6], the net pneumatic force is expressed as a non-linear function of the shock absorber stroke.
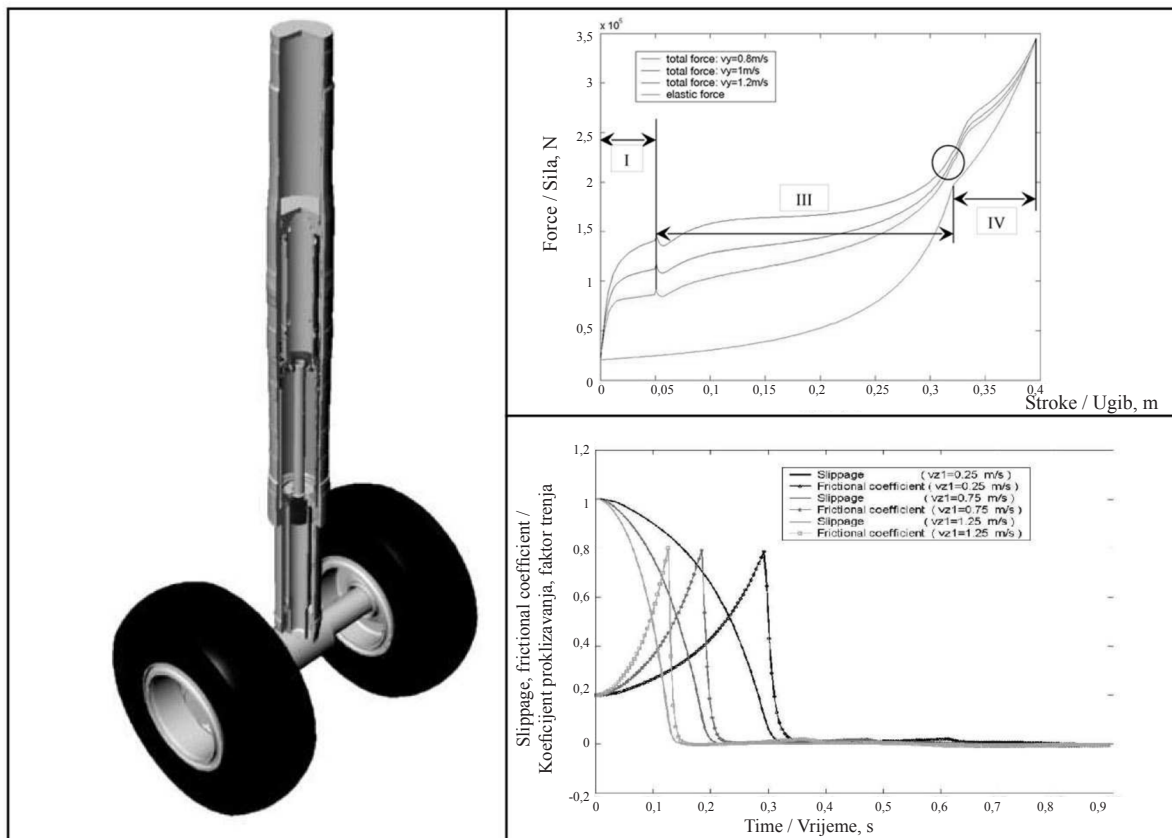
Figure 4. Main gear elastic leg - shock absorber load characteristics and variable slip-friction characteristics of tire contact spin-up force.

Slika 4. Elastična noga glavnog podvozja – karakteristika opterećenja elastično-prigušnog elementa i promjenjiva značajka sile trenja kontaktne dinamike gume.

3.1.2. *Hydraulic damping force*

The hydraulic damping force results from the pressure difference associated with the flow through the system of orifices. It is assumed that jet velocities and Reynolds numbers are sufficiently large for the flow to be fully turbulent (the orifice area is small in relation to the absorber diameter) [6]. As a result, the net damping force is expressed as a function of the stroke velocity. Since during the compression stroke some orifices become active/inactive (orifices K3 change their position as the absorber closes), the net hydraulic damping force is modelled via two stage discontinuous function of the absorber stroke velocity (Figure 4).

The orifice hydraulic resistance damping coefficients K1, K2, K3 (Figure 3) are estimated on the basis of orifice geometry and hydraulic fluid density according to [6]. Prior to dynamic simulations of landing aircraft, the dynamic model of shock absorber has been validated by numerical dynamic simulations (Figure 3) of landing gear drop test ([1] paragraphs 25.723-25.727).

4. Dynamic simulation procedures and numerical test cases

The schematic layout of dynamic simulator "global" architecture is shown in Figure 5. The dynamic simulator is modularly designed: numerical algorithms and procedures for dynamic response determination of different structural subsystems are decoupled during development.

They are independently validated on the basis of measurements taken on the airplane and characteristic data provided by manufacturer. After partial numerical tests are successfully performed (for example, numerical tests of main elastic leg dynamic characteristics, Fig. 2), the algorithms that control particular assembly units are mutually coupled and incorporated into the global simulation procedures, where additional tests and data validation are made for the whole system.

On the basis of the aircraft dynamic model, dynamic simulations of landing cases of large transport aircraft were performed for different initial descent velocities and
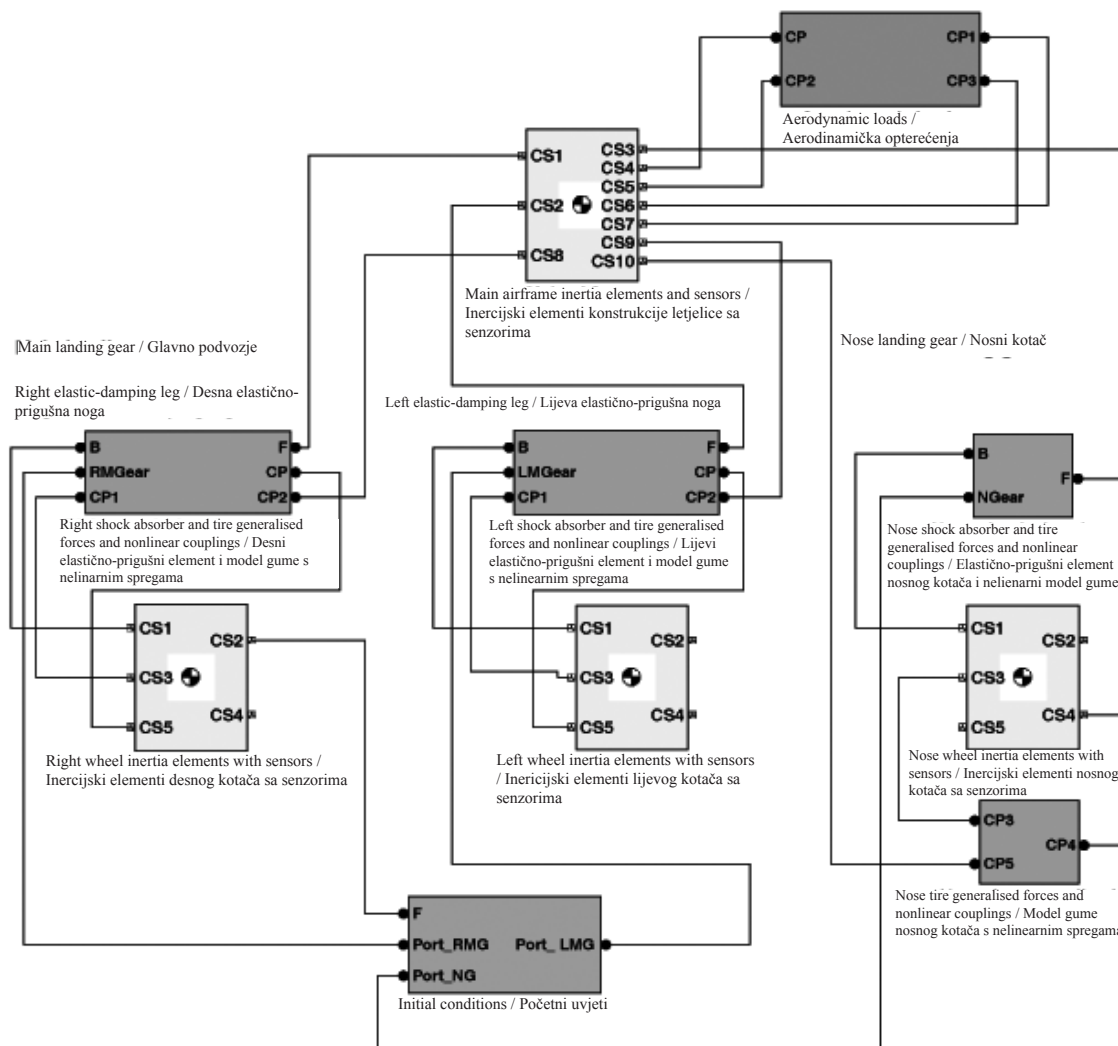
Figure 5. The schematic layout of dynamic simulator "global" architecture.

Slika 5. Shema dinamičkog simulatora globalne arhitekture.

lateral wind condition. The mass of the aircraft is set as 64500 kg and the horizontal velocity equals V_{x1} m/s. The initial aircraft pitch and roll angles prior to touchdown are 10° and 3° respectively, while the aircraft pitching and rolling velocity at the instant of touchdown is assumed to be approximately zero. The animation sequence of landing airplane is shown in Figure 6. Time evolution of the shock absorber stroke and total force in the left and right elastic leg during different landing cases, when descent velocity varies in the range from $V_{z1} = 0,25$ m/s to $V_{z1} = 1,25$ m/s is presented in Figure 7. - Figure 10.

The landing cases with the indicated touchdown parameters do not represent demanding landing scenarios for a modern transport airplane. During simulated landing impacts the absorber stroke time evolution is well within the range of 0,45 m (max. stroke) and no upper-point cylinder-piston collision occurred during analysed landing cases (which does not mean that stick-slip transitions cannot occur within shock-absorber mechanism). The undercarriage load factors are also well in the prescribed range.


Figure 6. The animation sequence of landing airplane with present lateral wind - one gear landing case.

Slika 6. Animacija slijetanja zrakoplova s prisutnim bočnim vjetrom – slijetanje na jednu elastičnu nogu glavnog podvozja.

It is evident that time diagrams of the shock absorbers' stroke and total force evolution are almost flat immediately after the touchdown. This is due to the fact that, since the shock absorber pneumatics act as a set-up spring, they are still not active during this period and the tire dynamics affect the overall system motion dominantly. This is more emphasised for the lower initial descent velocities.

In the cases of landing impacts with larger touchdown descent velocities the set-up value is quickly reached and damping hydraulic component builds up very fast after the impact, provoking thus a big gradient of the absorber total force soon after the moment of touchdown. Of course, left shock absorber values have an additional time delay due to the fact that the left elastic leg comes in to contact with the ground later on during the landing process, depending on the aircraft geometry and rolling motion.

The discontinuities visible at the shock absorber total force characteristics in Figure 7. and Figure 9. are due to the orifices different working regime (inactive/active K3 orifices, Figure 3, Figure 4) and due to the change of the absorbers' pneumatic force at the point where the floating piston of the second-stage pneumatic cylinder becomes active (Figure 4.).
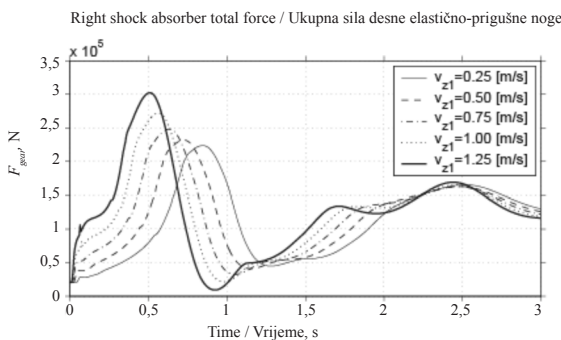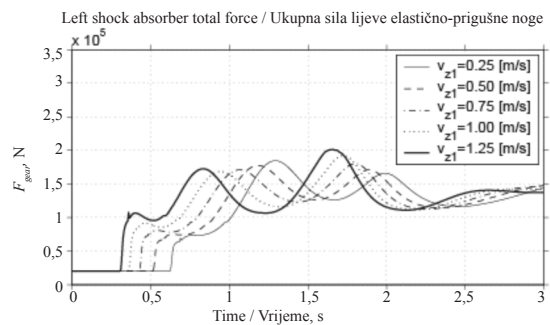

Figure 7. Shock absorber total force vs time (right elastic leg).
Slika 7. Ukupna sila elastično-prigušnog elementa u ovisnosti o vremenu (desna elastična noga).
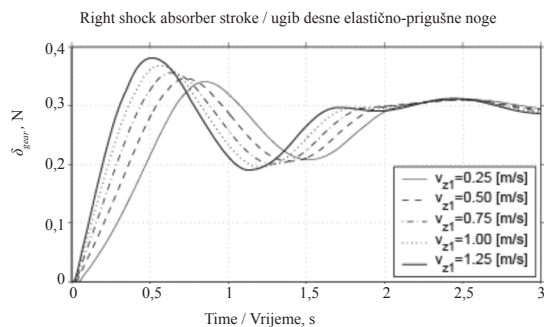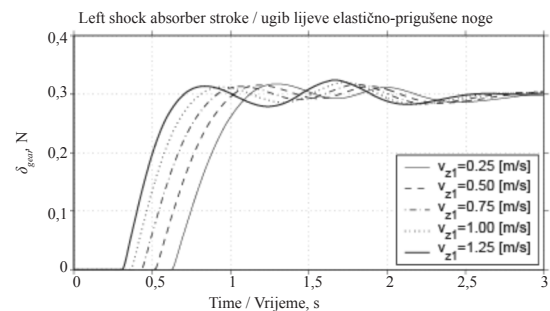

Figure 8. Shock absorber stroke vs time (right elastic leg).
Slika 8. Ugib elastično-prigušnog elementa u ovisnosti o vremenu (desna elastična noga).

5. Conclusion

As presented briefly here, a numerical simulaton algorithm of landing aircraft is based on dynamic response determination of the modelled aircraft for specified initial conditions, airplane aerodynamic data and runway contact loads. The aircraft dynamic model is designed as a multibody system with detailed non-linear dynamic model of landing gear assembly. Numerical simulaton procedures are modularly designed and dynamic models and algorithms of different structural subsystems (landing gear assembly, for example) are independently validated on the basis of technical documentation, JAA requirements and measured data. The airplane 3D aerodynamic model is estimated and used for dynamic simulation of landing approach in order to define initial conditions for aircraft multibody simulations after touch-down. The aerodynamic model is also used for determination of aerodynamic loads during system numerical simulation after touch-down and during taxiing.

Figure 9. Shock absorber total force vs time (left elastic leg).
Slika 9. Ukupna sila elastično-prigušnog elementa u ovisnosti o vremenu (lijeva elastična noga).

Figure 10. Shock absorber stroke vs time (left elastic leg).
Slika 10. Ugib elastično-prigušnog elementa u ovisnosti o vremenu (lijeva elastična noga)

The described, full-scale, non-linear multibody approach with detailed landing gear dynamic model and 3D aerodynamics, allows for a realistic estimation of aircraft dynamic loadings during landing with different flight parameters. It is expected that developed aircraft

model and computational algorithms can successfully serve as a core of flight navigation procedure trainer for different landing routines, provided that additional "man-in-the-loop" flight control routines are incorporated in the simulation procedures.

Acknowledgments

REFERENCES

[1] Joint Aviation Requirements, JAR-25, Large Aeroplanes, 1996.

[2] CHESTER, D. H.: *Aircraft landing impact parametric study with emphasis on nose gear landing conditions*, Journal of Aircraft, 39, (2002), 394-403.

[3] LOMAX, T. L.: *Structural Loads Analysis for Commercial Transport Aircraft: Theory and Practice*, AIAA, Educational series edition, 1996.

[4] WAPENHANS, H.: *Dynamik und Regelung von Flugzeugfahrwerken*, Institut und Lehrstuhl B für Mechanik, Technische Universität München, 1989.

[5] SMILEY, R. F. and HORNE, W. B.: *Mechanical properties of pneumatic tires with special reference to modern aircraft tires*, Technical report no. 4110, NACA, 1958.

[6] Airbus Industrie, Aircraft maintenance manual A319/A320, 2001.

[7] PFEIFER, F. and GLOCKER, C.: *Multibody Dynamics with Unilateral Contact*. John Willey & Sons, New York, 1996.

[8] TERZE, Z. et al.: *Null space integration method for constrained multibody system simulation with no constraint violation*, Multibody System Dynamics, 6, (2001), 229-243.

[9] TERZE, Z.; JANKOVIĆ, S. and VRDOLJAK, M.: *Estimation of input data for landing aircraft dynamic simulation: Aerodynamic loads and landing gear parametars*, Technical report TP-01/0120-01/KS, Dept. of Aeronautical Eng., F. Mech. Eng. Naval Arch., 2006. (in Croatian).

[10] HOAK, D. E. et al.: *The USAF stability and control – DATCOM*, TR-83-3048, Air Force Wright Aeronautical Laboratoties, 1960, Revised 1978.

[11] CURREY, N. S.: *Aircraft Landing Gear Design: Principles and Practices*. AIAA, Education series edition, 1988.

[12] MILWITZKY B. and COOK, F. E.: *Analysis of landing gear behaviour*, Technical report no. 1154, NACA, 1953.

[13] KAPADOUKAS, G. and SELF, A.: *The simulation of aircraft landing gear*, System Analysis Modelling Simulation, 21, (1995), 237-245.

[14] YADAV D. and RAMAMOORTHY, R. P.: *Nonlinear landing gear behaviour at touchdown*, Journal of Dynamic Systems, Measurement, and Control, 113, (1991), 677-683.